PROCEEDINGS of the
23rd International Congress on Acoustics
9 to 13 September 2019 in Aachen, Germany

Efficient Evaluation of Sound Radiation of an Electric Motor using Model Order Reduction

Martin ESER[(1)], Caglar GÜRBÜZ[(1)], Lennart MOHEIT[(1)], Marold MOOSRAINER[(2)] and Steffen MARBURG[(1)]

[(1)]Technical University of Munich (TUM), Germany, m.eser@tum.de
[(2)]CADFEM GmbH, Germany, mmoosrainer@cadfem.de

Abstract

Electric motors can suffer from severe noise radiation when the internal electromagnetic forces excite a natural vibration mode of the stator pack. These critical operation points can be identified from a Campbell diagram. The generation of the diagram based on numerical analyses is computationally very costly, in particular when the motor is to be analyzed in the mid-frequency range. The complex vibration behavior of the motor housing prohibits a straight-forward application of common model reduction processes. Therefore, a new multiple-input-multiple-output model reduction process is developed using the moment matching method based on Krylov subspaces. The in-vacou surface velocity modes of the motor housing yield as input load patterns. A structure-preserving second-order Arnoldi algorithm is used for the calculation of the Krylov subspaces. The proposed process enables the direct evaluation of the radiated sound power for all considered frequency points within a frequency band. The reduction process incorporates an adaptive selection of structural modes in order to allow for an efficient evaluation of the radiated sound power of the electric motor.

Keywords: Electric motor, Sound radiation, Model order reduction, Krylov subspace

1 INTRODUCTION

During the last decades, electrification of mobile systems has progressed consistently. Nowadays, there is broad variety of applications for electric motors: in the automotive industry [6, 2], for marine propulsion [7] or aircraft propulsion [12] and further applications [8, 3, 4]. The major advantages of an electric motor compared to a conventional internal combustion motor are improved fuel economy, reduced harmfull emissions and lower audible noise [12]. Due to the increasing importance of electric motors, many manufacturers integrate the production of electric motors into their value chain [6]. However, electric motors can suffer from severe noise radiation when the electromagnetic forces excite a natural vibration mode of the stator stack. Therefore, it is important to estimate the electromagnetic, structural dynamic and acoustic behavior of the motor early on the design process. The multiphysics problem concerning the noise emission of electric motors is modeled with three weakly-coupled modules: Electromagnetics, structural dynamics and acoustics, as displayed in figure 1.
Wibbeler *et al.* [11] developed a basic procedure for the solution of the multiphysics noise emission problem of an electric motor by use of the commercial finite element method (FEM) simulation environment of ANSYS. The basic procedure incorporates the electromagnetic analysis (module 1), in which the time-dependent electromagnetic forces are determined and the structural dynamics analysis (module 2).

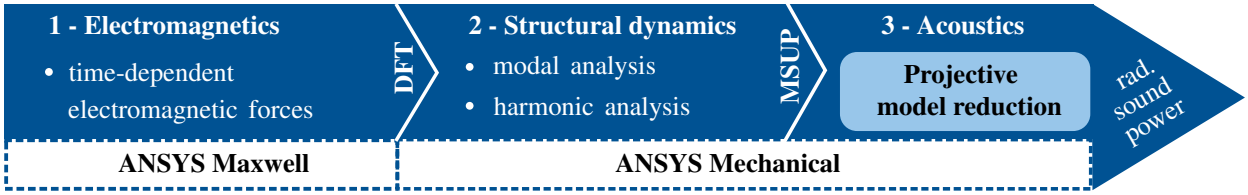

Figure 1. Simulation workflow of the weakly coupled multiphysics problem of the electric motor.

The electromagnetic forces are transferred to the frequency domain by use of a discrete Fourier transformation (DFT) and yield as excitation for the structural dynamics analysis. The modal superposition technique (MSUP) is used to solve the structural dynamics problem. In the basic framework, the acoustically radiated sound power for the Campbell diagram is approximated in terms of the equivalent radiated power, which solely encounters structure-borne noise and omits the frequency dependence of the radiation efficiency.
Jegham *et al.* [5] extend the basic procedure for a full-harmonic acoustic analysis (module 3) in order to obtain more realistic results regarding the noise emission of the electric motor. In acoustic problems, the computation effort and simulation times increase drastically with increasing frequency of interest. Jegham *et al.* overcome long calculation times, especially in the mid-frequency range, by use of high performance computation approaches, i.e. optimized balancing between mesh domain decomposition (MDD) and frequency domain decomposition (FDD).
This work presents an alternative approach to enable a fast and reliable acoustic analysis (module 3) for the generation of a Campbell diagram of an electric motor. The time-harmonic acoustic problem for an inviscid fluid, such as the air surrounding the motor, can be expressed in terms of the homogeneous Helmholtz equation

$$c^2 \Delta p + \omega^2 p = 0, \text{ in } \Omega. \tag{1}$$

Herein c and ω represent the speed of sound and the angular frequency and p is the generally sought sound pressure in the fluid domain of infinite extent Ω. The Laplace operator is expressed by Δ, representing the double derivative with respect to the spatial coordinates $\vec{x}$.

2 PROJECTIVE MODEL REDUCTION

The presented alternative approach for the efficient evaluation of the radiated sound power relies on the fundamentals of projective model reduction. In projective model reduction, the original system of equations (size $N \times N$) is projected onto to a system of reduced order (size $r \times r$) with way less degrees of freedom (DOFs), while maintaining the dynamic behavior of the system with a certain accuracy. An appropriate projection matrix $\boldsymbol{V} \in \mathbb{C}^{N \times r}$ is used for this purpose. The reduced-order acoustic system is obtained from the application of the projection matrix onto the FEM-discretized Helmholtz equation [10]

$$\left(\boldsymbol{K} + j\omega\boldsymbol{D} - \omega^2\boldsymbol{M}\right)\vec{p} = \vec{F} \quad \xRightarrow[N>>r]{\text{projection}} \quad \left(\boldsymbol{K}_r + j\omega\boldsymbol{D}_r - \omega^2\boldsymbol{M}_r\right)\vec{p}_r = \vec{F}_r. \tag{2}$$

The stiffness, damping and mass matrix of the original system are denoted by $\boldsymbol{K}$, $\boldsymbol{D}$ and $\boldsymbol{M}$ respectively. $\vec{F}$ stands for the acoustic load vector of original dimension. The imaginary unit is represented by $j = \sqrt{-1}$. The system matrices of reduced order in equation 2 are given by [10]

$$\boldsymbol{M}_r = \boldsymbol{V}^T\boldsymbol{M}\boldsymbol{V}, \ \boldsymbol{D}_r = \boldsymbol{V}^T\boldsymbol{D}\boldsymbol{V}, \ \boldsymbol{K}_r = \boldsymbol{V}^T\boldsymbol{K}\boldsymbol{V}, \ \vec{F}_r = \boldsymbol{V}^T\vec{F}. \tag{3}$$

Instead of solving for the original column matrix of discrete sound pressure values $\vec{p} \in \mathbb{C}^N$, the system of equations 2 is solved for the state vector of reduced dimension $\vec{p}_r \in \mathbb{C}^r$, with $r << N$, such that $\vec{p} \approx \boldsymbol{V}\vec{p}_r$ [10]. The moment matching method based on Krylov subspaces is applied in order to define the projection subspace. This method relies on the local approximation of the input-output transfer function of the acoustic system within a given frequency range. Equation 2 of the original system has to be reformulated according to system theory in order to allow for the application of the moment matching method, i.e. [10]

$$\vec{p} = \boldsymbol{C}^T\left(\boldsymbol{K} + j\omega\boldsymbol{D} - \omega^2\boldsymbol{M}\right)^{-1}\vec{b}v(\omega) \quad \xRightarrow[N>>r]{\text{projection}} \quad \vec{p}_r = \boldsymbol{C}_r^T\left(\boldsymbol{K}_r + j\omega\boldsymbol{D}_r - \omega^2\boldsymbol{M}_r\right)^{-1}\vec{b}_r v(\omega). \tag{4}$$

In equation 4, the acoustic load vector is decomposed into a constant, frequency independent load pattern $\vec{b}$ and a frequency dependent scalar factor $v(\omega)$. This decomposition is essential for the successful application of the presented model reduction method. Furthermore an output matrix $\boldsymbol{C}$ is introduced. It enables the selection

of specific, predefined DOFs, that are scope of the analysis. In case of a single-input-single-output system, the output matrix degenerates to a vector of zeros with one single unity entry at the corresponding position of the desired DOF. The corresponding reduced-order output matrix and load pattern are given by [10]

$$\boldsymbol{C}_r = \boldsymbol{V}^T \boldsymbol{C},\ \vec{b}_r = \boldsymbol{V}^T \vec{b}. \tag{5}$$

Choice of Projection Matrix

The moment matching method is based on the approximation of the transfer function of the original system as well as the transfer function of the reduced system in terms of a Padé-type approximation. Both function approximations are carried out around the same expansion point ω_0. The first r moments of both transfer functions match, if the columns of the used projection matrix span a particular Krylov subspace $\mathbb{K}$ of order r [1]. The Krylov subspace is calculated by use of the second-order Arnoldi (SOAR) algorithm [1, 9]. As a result, an orthonormal set of r Krylov vectors $\vec{\kappa}$ is generated, spanning the second-order Krylov subspace of order r [1]

$$\mathbb{K}\left(\boldsymbol{K}, \boldsymbol{D}, \boldsymbol{M}, \vec{b}\right) = \mathrm{span}\left(\vec{\kappa}_0, \vec{\kappa}_1, ..., \vec{\kappa}_{r-1}\right) \Longrightarrow \boldsymbol{V} = \left\{\vec{\kappa}_0, \vec{\kappa}_1, ..., \vec{\kappa}_{r-1}\right\}. \tag{6}$$

The resulting set of Krylov vectors is further used as the projection matrix for the model reduction process. The load pattern vector $\vec{b}$ is explicitely considered for the calculation of the starting vector $\vec{\kappa}_0$. This fact demonstrates the necessity of a frequency independent load pattern. The desired output can hence be efficiently calculated for various frequencies of interest through the reduced form of equation 4.

3 DEVELOPMENT OF NOVEL MODEL REDUCTION PROCESS

The load pattern of an electric motor varies with the frequency and additionally with the rotational speed of the motor. As a consequence, the application requirement for the model reduction process of a constant load pattern is not given anymore. The model reduction process, as presented in the previous section, cannot be directly applied under these circumstances.

3.1 Multiple-Input Extension Approach

The system theory formulation of the original system (eq. 4) can be extended for multiple inputs (number of inputs M) [10]

$$\vec{p} = \boldsymbol{C}^T \left(\boldsymbol{K} + j\omega\boldsymbol{D} - \omega^2\boldsymbol{M}\right)^{-1} \boldsymbol{B}\vec{v}(\omega). \tag{7}$$

In this case, the acoustic load vector is decomposed into multiple constant, frequency independent load patterns and a corresponding vector of corresponding scalar, frequency dependent factors $\vec{v}(\omega)$. The load patterns are arranged columnwisely in the load pattern matrix. The modal properties of the structure are analyzed in the previous analysis module of the multiphysics approach (cf. structural dynamics in fig. 1). The eigenmodes of the radiating surface $\vec{\phi}_m(\vec{x})$ represent potential load patterns for equation 7, as they are independent of the frequency and of the rotational speed. The load pattern matrix of the electric motor hence results in

$$\boldsymbol{B} = \left\{\vec{\phi}_1(\vec{x}), \vec{\phi}_2(\vec{x}), ..., \vec{\phi}_M(\vec{x})\right\}. \tag{8}$$

The vector of frequency dependent factors is given by the complex-valued modal coefficients, which result from the harmonic analysis of the structure (cf. module 2 in fig. 1), i.e.

$$\vec{v}(\omega) = \left\{v_1(\omega), v_2(\omega), ..., v_M(\omega)\right\}. \tag{9}$$

The load pattern problem of the electric motor is solved through this approach. However, the radiated sound power P is the quantity of interest for the generation of the Campbell diagram. The radiated sound power can be directly calculated from the state-space system formulation (eq. 7) by adapting the coefficients of the output

matrix. For a specific frequency of interest ω_k, the coefficients of the corresponding column in the adapted output matrix $\hat{C}_{:,k}$ follow from the acoustic load vector in terms of

$$\hat{C}_{:,k} = j/\left(\rho_f \omega_k\right) \vec{F}^*\left(\omega_k\right). \tag{10}$$

$\vec{F}^*$ indicates the conjugate complex of the acoustic load vector for the corresponding frequency and ρ_f represents the density of the air. For the consideration of for multiple frequencies of interest, the vector of scaling factors needs to be extended to a matrix of scaling factors $\boldsymbol{Y}$. This matrix is constructed by columnwise concatenation of all vectors of modal coefficients. The column in the matrix of scaling factors, which corresponds to a specific frequency ω_k is given by

$$Y_{:,k} = \vec{v}\left(\omega_k\right). \tag{11}$$

Introducing the adapted output matrix (eq. 10) and the extended matrix of scaling factors (eq. 11) into equation 7, the radiated sound power can be evaluated for each considered frequency point in the frequency interval of interest according to

$$\vec{P} = \left\{P\left(\omega_1\right), ..., P\left(\omega_k\right), ..., P\left(\omega_{nfrq}\right)\right\} = 1/2 \ \mathrm{Re}\left\{\mathrm{diag}\left\{\hat{\boldsymbol{C}}^T \left(\boldsymbol{K} + j\omega\boldsymbol{D} - \omega^2\boldsymbol{M}\right)^{-1} \boldsymbol{B}\boldsymbol{Y}\right\}\right\}. \tag{12}$$

Application of the moment matching method based on Krylov subspaces with the SOAR algorithm onto the equation 12, leads to the final system of reduced order

$$\vec{P} \approx 1/2 \ \mathrm{Re}\left\{\mathrm{diag}\left\{\hat{\boldsymbol{C}}_r^T \left(\boldsymbol{K}_r + j\omega\boldsymbol{D}_r - \omega^2\boldsymbol{M}_r\right)^{-1} \boldsymbol{B}_r\boldsymbol{Y}\right\}\right\}, \ \text{with} \ \hat{\boldsymbol{C}}_r = \boldsymbol{V}^T\hat{\boldsymbol{C}}, \boldsymbol{B}_r = \boldsymbol{V}^T\boldsymbol{B}, \tag{13}$$

which is evaluated for each frequency point within the frequency range of interest. Due to the consideration of multiple load patterns, multiple Krylov subspaces have to be calculated in order to define the global projection matrix for the projection of equation 12. The global projection matrix V follows from the concatenation of all Krylov subspaces, or in other words, the columnwise concatenation of all Krylov vectors as

$$\boldsymbol{V} = \left\{\mathbb{K}^{(1)}, ..., \mathbb{K}^{(m)}, ..., \mathbb{K}^{(M)}\right\} = \left\{\vec{\kappa}_0^{(1)}, ..., \vec{\kappa}_{r-1}^{(1)}, ..., \vec{\kappa}_0^{(m)}, ..., \vec{\kappa}_{r-1}^{(m)}, ..., \vec{\kappa}_0^{(M)}, ..., \vec{\kappa}_{r-1}^{(M)}\right\}, \ \text{with} \ m = 1, 2, ..., M. \tag{14}$$

The superscript (m) denotes the correspondence of the Krylov vectors to the respective Krylov subspace. One Krylov subspace of prescribed order r is calculated by use of the SOAR algorithm for each load pattern. This correlation is displayed in figure 2.

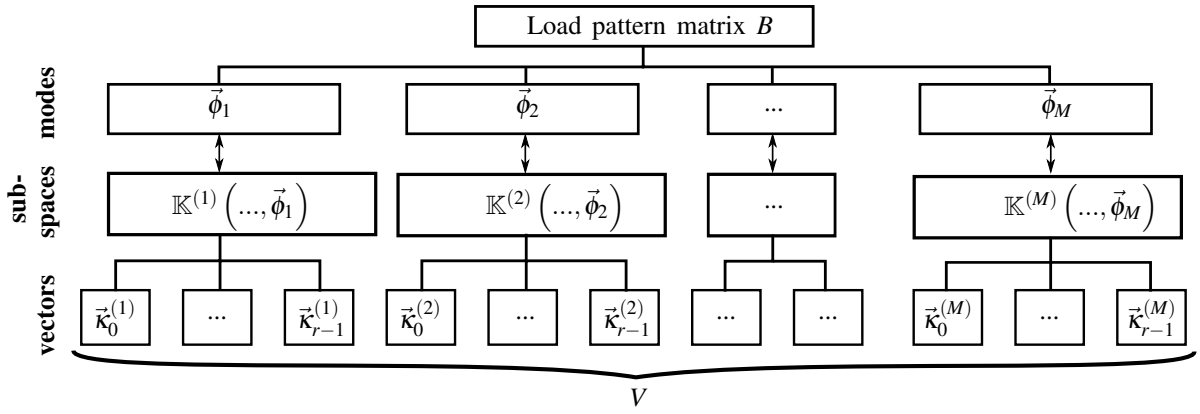

Figure 2. Tree diagram for the multiple input reduction process of the electric motor.

4 ELECTRIC MOTOR ANALYSIS

In the structural dynamics analysis, the undamped modes are calculated up to a maximum frequency of 20000 Hz. The motor structure is discretized with an unstructured mesh with quadratic tetrahedral elements. The motor housing is supposed to be fixed to an artificial ground. The dynamic response of the motor structure is calculated in the consecutive structural harmonic response analysis under consideration of a constant damping ratio of $\xi = 0.002$. The Fourier-transformed electromagnetic forces, which are already given from previous work [11], yield as excitation. The first 30 rotational speed orders of five excitation spectra ($n_{\text{rot}} = 1500, 6000, 9000, 12000$ and 20000 rpm) are considered in this case. The structural harmonic response is calculated for an operation speed of 500 to 5000 rpm and in a frequency range from 30 to 10000 Hz. The results of the structural dynamics analysis are passed to the harmonic acoustics analysis, which is carried out for a frequency range of 30 to 5000 Hz. This frequency range is split into four frequency intervals $f^{(i)}$, guaranteeing moderate sizes of the original system. The bounds of the considered frequency intervals and additional analysis parameters are listed in table 1. The maximum acoustic frequency leads to a consideration of 75 structural modes for the acoustic analysis, according to the common rule of thumb for modal superposition. A spherical half-space is considered for the acoustic analysis. The acoustic domain is discretized with tetrahedral elements of quadratic order with a resolution of six elements per minimum wavelength of each frequency interval. The Sommerfeld radiation condition is considered by use of absorbing elements (FLUID130) on the truncated domain boundary. In total, 912 calculation points are considered for the generation of the Campbell diagram of the electric motor demonstrator. The considered motor geometry is displayed in figure 3.

Table 1. Frequency intervals and corresponding data for the acoustic analysis of the electric motor.

frequency interval (Hz)	$f^{(1)}$: 30-300	$f^{(2)}$: 300-1800	$f^{(3)}$: 1800-3200	$f^{(4)}$: 3200-5000
calculation points	74	396	239	203
DOFs	301681	276033	251515	371521
subspace order	50	55	65	80

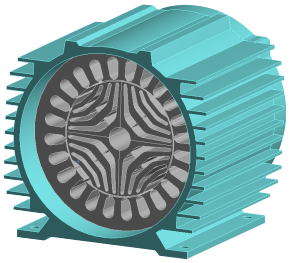

Figure 3. CAD sketch of the analyzed electric motor with supressed front cap.

A full-harmonic acoustic analysis with MDD yields the reference solution (subscript "ref"). The expansion point for the model reduction process is located at the average value of each frequency interval. The analysis of the electric motor is carried out using ANSYS Mechanical v.19.1 on a computer with Windows 8 operation system and 120 GB RAM. 8 physical cores are used for parallel computation.

4.1 Campbell Diagram and Accuracy

The sound power results of the reduced-order model analysis of the electric motor are displayed in the Campbell diagram in figure 4. Critical operation points can be identified from this diagram as exemplarily indicated. The first eigenmode of the motor housing is excited at the indicated critical operation point. The application of the developed model reduction procedure enables the complete evaluation of all radiated sound power values, while reducing the total calculation time by approximately 35 % compared to the full-harmonic reference solution. The accuracy of the results of the reduced-order model is exemplarily analyzed at specific rotational speed points. The considered rotational speed points ($n_{\text{rot}} = 500, 2250$ and 4500 rpm) are marked in the Campbell diagram with dashed black lines. The accuracy is evaluated in terms of the absolute error in the radiated sound power level between the reduced-order model solution and the reference solution

$$|\Delta L_W|_{\text{abs}} = |L_W - L_{W,\text{ref}}|. \tag{15}$$

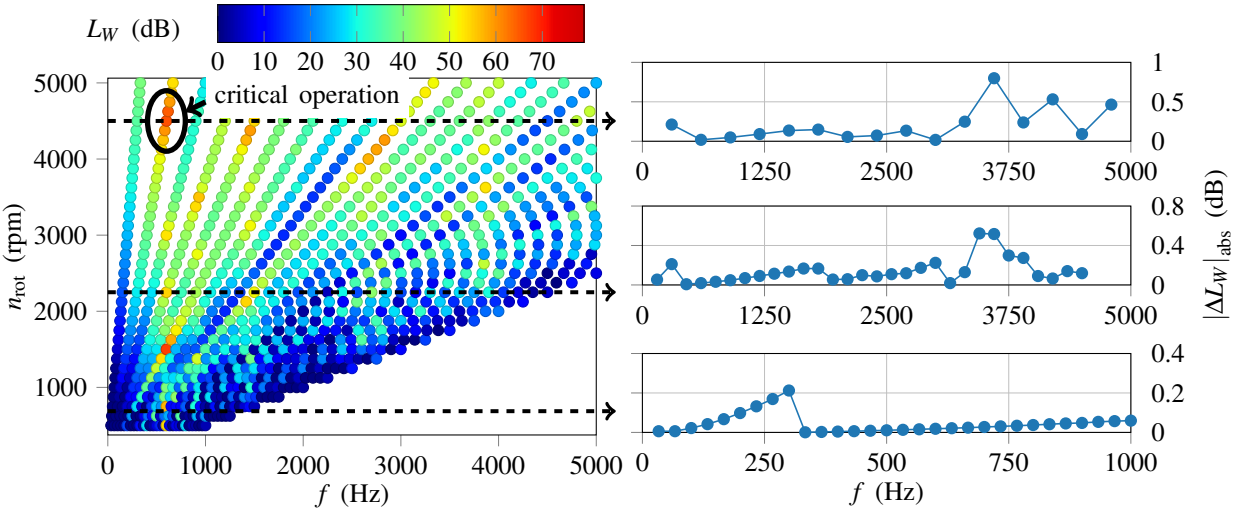

Figure 4. Waterfall diagram of the reduced-order model of the electric motor for a rotational speed range of 500 to 5000 rpm and a frequency range of 0 to 5000 Hz.

Figure 5. Absolute error in sound power level $|\Delta L_W|_{\mathrm{abs}}$ in dB at specific rotational speed points: Lower graph $n_{\mathrm{rot}} = 500$ rpm, middle graph $n_{\mathrm{rot}} = 2250$ rpm, upper graph $n_{\mathrm{rot}} = 4500$ rpm.

The absolute error in the sound power level is shown in figure 5 for the chosen rotational speed points. The reduced-order model shows good accuracy for all considered rotational speed points. A maximum error below 0.8 dB over the whole operation range is absolutely viable for industrial applications, as sound power level variations below 1 dB cannot be perceived by humans. The increase in the maximum error with the frequency is a result of the more complex radiation behavior of the electric motor at higher frequencies. Due to the fixed number of Krylov vectors per frequency interval, the approximation capability of the reduced-order transfer function is limited in accuracy in each frequency interval. The number of Krylov vectors is increased for each frequency interval in order to ameliorate the transfer behavior approximation at higher frequencies (cf. tab. 1).

4.2 Composition of Reduced Model Calculation Time

The number of calculation points in a frequency interval as well as the number of Krylov vectors per load pattern has a significant influence on the duration of the solution process of the reduced-order model. The relative calculation times of the solution process of are analyzed in the following in order to highlight possible optimization potential of the presented approach. While the adapted output matrix $\hat{\boldsymbol{C}}$ is calculated in a preprocessing step, the reduced-order model solution process can be split into five steps:

- Decomposition of the frequency range of interest into frequency intervals (split frq. range)
- Generation of the load pattern matrix $\boldsymbol{B}$ (generation of $\boldsymbol{B}$)
- Generation of the matrix of scaling factors $\boldsymbol{Y}$ (generation of $\boldsymbol{Y}$)
- Projection process with by the global projection matrix $\boldsymbol{V}$; this step includes the LU-decomposition, the calculation of the Krylov vectors and the actual projection process (projection)
- Evaluation of the radiated sound power with equation 13 (evaluation of L_W)

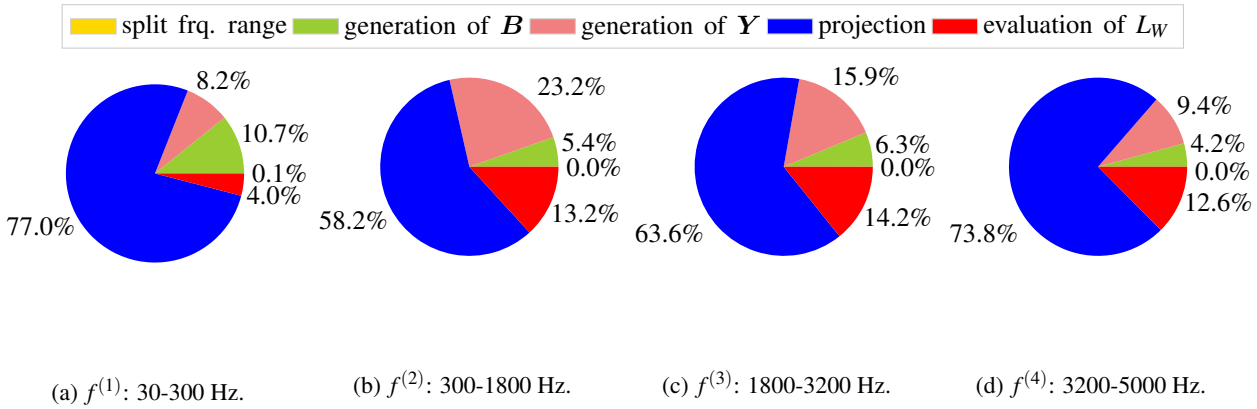

(a) $f^{(1)}$: 30-300 Hz. (b) $f^{(2)}$: 300-1800 Hz. (c) $f^{(3)}$: 1800-3200 Hz. (d) $f^{(4)}$: 3200-5000 Hz.

Figure 6. Relative elapsed time of the substeps forming the MOR solution process (MORsolve) for the harmonic acoustic analysis of the electric motor demonstrator displayed for each frequency interval.

The relative calculation times of the above mentioned solution steps are displayed for each frequency interval in figure 6. In case of the second and third frequency interval, a higher amount of time is needed for the generation of the matrix of scaling factors, due to the increased number of calculation points within these intervals (cf. tab. 1). An increased amount of time is as well observed for the final evaluation of the sound power level in the second, the third and the fourth frequency interval. On the one hand, the number of calculation points also affects this substep, as it defines the final dimension of the resulting output vector. On the other hand, the total size of the reduced system affects the time for this substep. The higher the maximum frequency of a frequency interval is, the more Krylov vectors have to be calculated for each input load pattern, due to accuracy reasons. The final evaluation of the sound power level takes more time for a reduced system of increased size. The projection process necessitates most of the solution time for all frequency intervals. This is due to the fact that one Krylov subspace of order r needs to be calculated for each individual input load pattern. The total number of Krylov vectors per frequency interval depends linearly on the number of considered structural modes and the chosen order for one Krylov subspace. This effect magnifies with increasing maximum frequency, as more structural modes have to be considered as load patterns. Furthermore, the number of Krylov vectors per load pattern has to be increased with the maximum frequency. This effect is well-displayed in the tree diagram for the developed model reduction process (cf. fig. 2).

5 CONCLUSION AND OUTLOOK

This work presents a method based on model reduction via the moment maching method with Krylov subspaces in order to analyze the noise emission of an electric motor. The method is validated against an electric motor demonstrator. The application of the method reduces the total time until the motor's Campbell diagram is obtained by approximately 35 % compared to a full-harmonic acoustic analysis, while maintaining a good level of accuracy. The relative calculation times for each substep of the solution process of the reduced-order method is analyzed to reveal further potential for optimization. The projection process itself takes most of the calculation time, as it incorporates the algorithm for calculating the Krylov vectors. An alternative, second-order structure-preserving block Arnoldi algorithm could be used to calculate the Krylov subspaces. To the authors' knowledge however, such a method does not exist yet. As all individual Krylov subspaces are independent of each other, a singular value decomposition of the global projection matrix could reveal for further potential for a deflation of the global projection space. This could reduce the overall size of the reduced system. A parallelized computation of individual Krylov subspaces could enable considerable time savings. By this, multiple subspaces are calculated at a time, instead of calculating each Krylov subspace sequentially.

REFERENCES

[1] Bai, Z.; Su, Y. Dimension reduction of large-scale second-order dynamical systems via a second-order Arnoldi method. SIAM Journal on Scientific Computing, Vol 26 (5), 2005, pp 1692-1709.

[2] Barkenbus, J. Our electric automotive future: CO_2 savings through a disruptive technology, Policy and Society, Vol 27 (4), 2009, pp 399-410.

[3] Bogusz, P.; Korkosz, M.; Prokop, J. The assessment of energy efficiency of electric machines for domestic appliances drive. E3S Web of Conferences, Vol 14, 2017, In CD-ROM.

[4] Hu, Y.; Liu, S.; Ileleji, K.; Mi, Y.; Han, L. Design and 3-dimension simulation of a mixed mode solar barn drier for drying wastewater sewage sludge. Thermal Science, Vol 22 (2), 2017, pp 419-427.

[5] Jegham, M.; Moosrainer, M. Mid-frequency challenge - efficient simulation of sound radiation of electric motors. Fortschritte der Akustik - 44. Jahrestagung für Akustik (DAGA), Munich, Germany, March 19-22, 2018, In CD-ROM.

[6] Kampker, A.; Kreisköther, K.; Büning, M. K.; Treichel, P.; Theelen, J. Automotive quality requirements and process capability in the production of electric motors. 2017 7th International Electric Drives Production Conference (EDPC), Würzburg, Germany, December 5-6, 2017, pp 1-8.

[7] Li, H.; Xie, H.; Xie, Y. Research on PMSM model predictive control for ship electric propulsion. 2018 Chinese Control And Decision Conference (CCDC), Shenyang, China, June 9-11, 2018, pp 1392-1398.

[8] Raja, R.; Sebastian, T.; Wang, M.; Chowdhury, M. Stator inductance estimation for permanent magnet motors using the PWM excitation. 2017 IEEE Energy Conversion Congress and Exposition (ECCE), Cincinnati, OH, USA, 2017, pp 3208-3214.

[9] Rudnyi, E. B.; Korvink, J. G. Model order reduction for large scale engineering models developed in ANSYS. In: Dongarra, J.; Madsen, K.; Wasniewski, J., Applied Parallel Computing. State of the Art in Scientific Computing, Springer, Berlin, Heidelberg (Germany), 2006.

[10] Van de Walle, A. The power of model order reduction in vibroacoustics - and its applications in model-based sensing, Dissertation, KU Leuven, Leuven, Belgium, 2018.

[11] Wibbeler, J.; Moosrainer, M.; Hanke, M. FEM-basierte Körperschallanalyse für elektrische Antriebe. Fortschritte der Akustik - 43. Jahrestagung für Akustik (DAGA), Kiel, Germany, March 6-9, 2017, In CD-ROM.

[12] Zhang, X.; Bowman, C. L.; O'Connell, T. C.; Haran, K. S. Large Electric Machines for Aircraft Electric Propulsion. IET Electric Power Applications, Vol 12 (6), 2018, pp 767-779.